MICROSTRUCTURE OF SWIFT HEAVY ION IRRADIATED SiC, Si_3N_4 AND AlN –

S.J. Zinkle, J.W. Jones (Oak Ridge National Laboratory) and V.A. Skuratov (Flerov Laboratory, Dubna, RF)

OBJECTIVE

The objective of this report is to determine the threshold ionizing radiation stopping powers for creation of displacement damage in ceramics of interest for fusion applications.

SUMMARY

Cross-section transmission electron microscopy was used to investigate the microstructure of single crystal silicon carbide and polycrystalline silicon nitride and aluminum nitride following room temperature irradiation with either 245 MeV Kr or 710 MeV Bi ions. The fluences ranged from $1x10^{12}/cm^2$ (single track regime) to $1x10^{13}/cm^2$. Ion track formation was observed in the Bi ion-irradiated Si_3N_4 specimen in regions where the electronic stopping power exceeded a critical value of ~15 keV/nm (depths <24 µm). Ion track formation was not observed at any depth in 245 MeV Kr ion-irradiated Si_3N_4, in which the maximum electronic stopping power was 14.5 keV/nm. There was no evidence for track formation in either SiC or AlN irradiated with 710 MeV Bi ions, which indicates that the threshold electronic stopping power for track formation in these two ceramics is >34 keV/nm. The high resistance of SiC and AlN to track formation may be due to their high thermal conductivity, but further study is needed to quantitatively evaluate the suitability of the various track formation models.

PROGRESS AND STATUS

INTRODUCTION

Previous studies have shown that discontinuous track formation in ceramic insulators can be produced by swift heavy ions with electronic stopping powers $(dE/dx)_e$ above ~5 to 8 keV/nm, and continuous cylindrical tracks are typically observed for $(dE/dx)_e \geq 15$ to 20 keV/nm [1]. These electronic stopping power thresholds for track formation are only slightly above the calculated electronic stopping powers associated with primary recoil atoms damage in ceramics in a fusion reactor environment. The physical mechanism(s) responsible for track formation in radiolysis-resistant solids are still under debate (e.g., thermal spike vs. Coulomb explosion models). Therefore, additional data on a wide range of materials are needed to investigate material parameters such as the effect of band gap energy and thermal conductivity on track radius, etc. As noted previously [2], it is possible that densely ionizing recoil atoms can create irradiated microstructures that are not achievable with conventional (elastic collision) irradiations. Therefore, materials which exhibit good radiation resistance under elastic collision damage conditions (e.g., $MgAl_2O_4$) may not necessarily exhibit similar radiation damage resistance under energetic recoil ion conditions [2]. This observation needs to be considered for the investigation of candidate in-vessel ceramic insulators for fusion reactors, due to the relatively high recoil ion energy for DT fusion neutrons.

Most previous swift heavy ion studies on ceramics have focussed on oxide insulators. Very little information is known about the behavior of carbides such as SiC [3-5], and even less is known about the behavior of nitride insulators such as AlN and Si_3N_4.

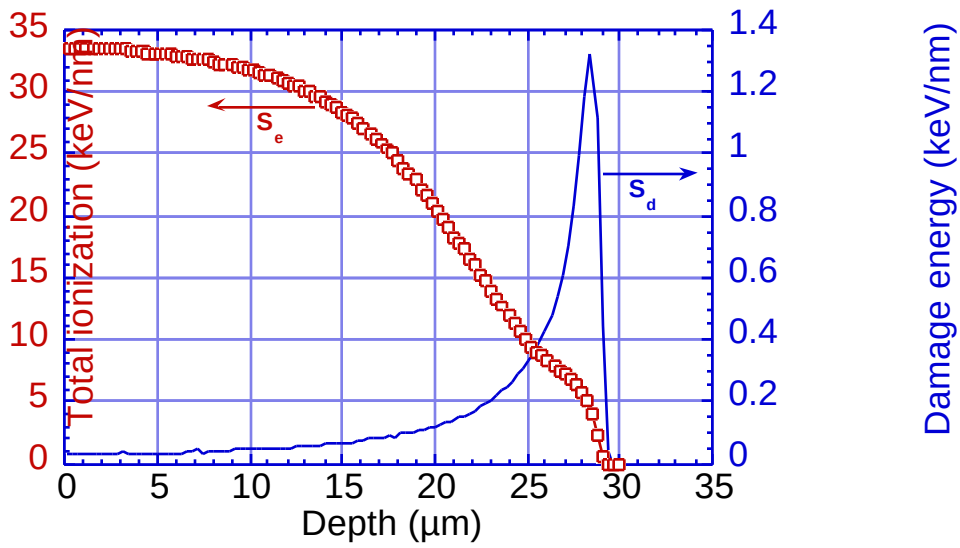

Fig. 1. Calculated damage energy (portion of nuclear stopping power that produces elastic collisions) and electronic stopping power (S_e) for 710 MeV Bi ions in Si_3N_4.

Table 1. Summary of room temperature properties of the investigated SiC, AlN and Si_3N_4 ceramics [7,8].

Material	Crystal structure	Lattice parameters	Density (g/cm^3)	Thermal conductivity (W/m-K)	Band gap (eV)	Ionicity	Sublimation temperature (K)
SiC (Cree)	Hexagonal (6H polytype)	a=0.308 nm c=1.512 nm c/a=4.91	3.21	350	3.0	0.12	2250
AlN (Tokuyama Shapal SH15)	Hexagonal (wurtzite)	a=0.311 nm c=0.498 nm c/a=1.60	3.31	177	6.2	0.40	2790
β-Si_3N_4 (Kyocera SN733)	Hexagonal ($P6_3$ space group)	a=0.760 nm c=0.290 nm c/a=0.290	3.21	29	~8	0.28	2151

EXPERIMENTAL PROCEDURE

Single crystal SiC (Cree) and polycrystalline specimens of AlN (Tokuyama Shapal grade SH15) and Si_3N_4 (Kyocera SN733, hot isostatically pressed) were irradiated at room temperature with either 245 MeV Kr or 710 MeV Bi ions at the Dubna U-400 cyclotron facility. The ion fluences ranged from $1x10^{12}$ ions/cm^2 (isolated track regime) to $1x10^{13}/cm^2$. The electronic stopping power (S_e) and displacement damage profiles were calculated using the TRIM2000 program [6]. Figure 1 shows the calculated results for 710 MeV Bi ions in Si_3N_4. The maximum displacement damage due to elastic collisions occurs at a depth of ~28 µm, and amounts to ~0.013 displacements per atom (dpa) for a fluence of $1x10^{13}/cm^2$, assuming a sublattice-averaged displacement energy of 40 eV. Similar profiles were calculated for Bi ions in SiC and AlN. Table 1 summarizes some of the room temperature physical parameters for the three ceramics.

Following irradiation, cross-section TEM specimens were prepared by gluing the irradiated disks to polished unirradiated disks, sectioning, grinding to 0.1 mm, dimpling to 20 µm, and then dual-gun ion beam thinning at ~80 K with 6 keV Ar ions until perforation occurred near the interface. The specimen surfaces were cleaned using 3 keV Ar ions at an angle of 11˚. The AlN and Si_3N_4 specimens were coated with a thin (~5 nm) layer of carbon prior to examination. The specimens were examined using conventional bright-field and dark-field imaging techniques in a Philips CM-30 microscope operating at 300 kV.

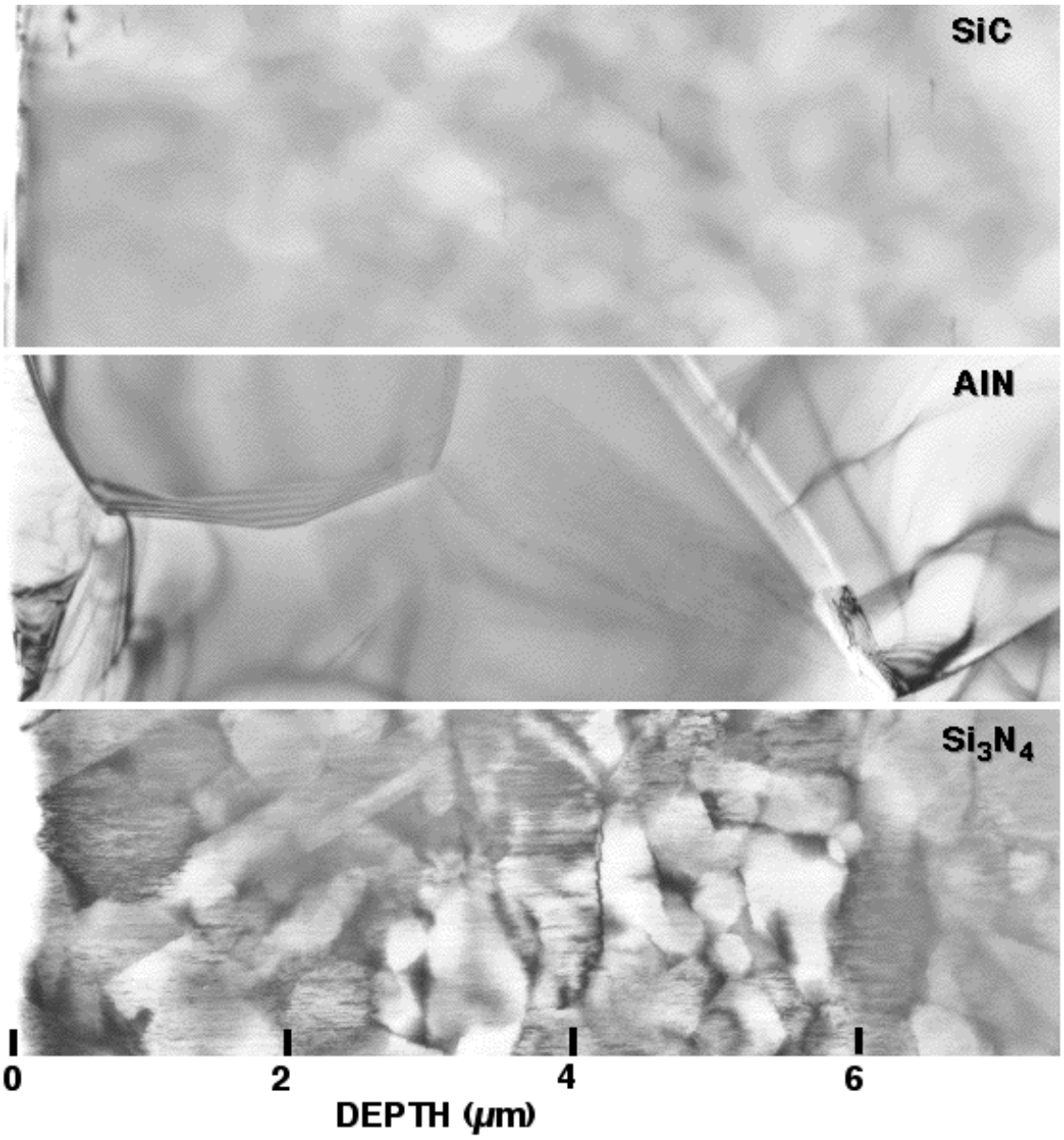

Fig. 2. Comparison of the low-magnification microstructures of SiC, AlN and Si_3N_4 irradiated with 710 MeV Bi ions.

RESULTS

Figure 2 compares the low-magnification bright-field cross-section microstructures of SiC, AlN and Si_3N_4 irradiated with 710 MeV Bi ions. The ion fluences were $1x10^{13}/cm^2$ for SiC and AlN, and $3x10^{12}/cm^2$ for Si_3N_4. Ion tracks were visible in the Si_3N_4 specimen even at low magnification. Conversely, ion tracks were not visible in the SiC and AlN specimens at any location along the ion beam path (bright field and dark field imaging up to 300 kx). The ion tracks in the Si_3N_4 specimen were visible from the irradiated surface to a depth of ~23 µm. This implies that the threshold electronic stopping power for track formation in Si_3N_4 is ~15 keV/nm for Bi ions.

Figure 3 shows a higher magnification view of the microstructure of the Si_3N_4 specimen irradiated with 710 MeV Bi ions to a fluence of $3x10^{12}/cm^2$. The ion track diameter was ~4.5 nm. A diffuse halo was observable in diffraction patterns taken from the ion track region of the specimen. Faint ion tracks could be imaged by centered dark field techniques, using the halo pattern. This implies that the center of the ion track is amorphous in the Si_3N_4 specimens irradiated with 710 MeV Bi ions. High resolution lattice imaging of an irradiated Si_3N_4 specimen (plan view) will be performed to conclusively determine whether or not the ion track center is amorphous.

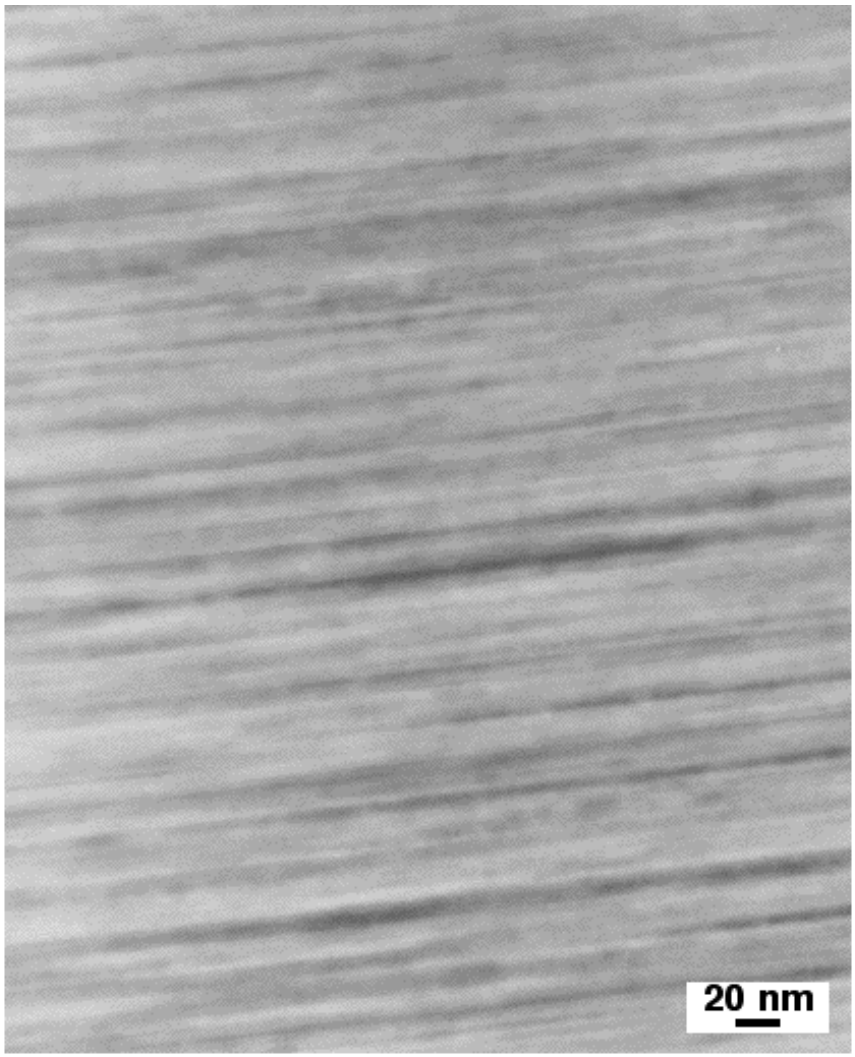

Fig. 3. Microstructure of Si_3N_4 irradiated with 710 MeV Bi ions.

In order to further investigate the threshold electronic stopping power for track formation in Si_3N_4, the microstructure of specimens irradiated with 245 MeV Kr ions to a fluence of $1x10^{13}/cm^2$ was examined. Although evidence for radiation damage to a depth of ~20 µm was visible in optical micrographs of a cross-section specimen, there was no evidence for ion track formation during extensive TEM examination. Ion tracks were also not observed in the SiC or AlN specimens irradiated with 245 MeV Kr ions.

Figure 4 compares the calculated depth-dependent electronic stopping powers for 710 MeV Bi and 245 MeV Kr ions in Si_3N_4. The maximum electronic stopping power for 245 MeV Kr ions is ~14.5 kV/nm, occurring at a depth of ~7 µm. Therefore, the absence of visible ion tracks in Si_3N_4 irradiated with 245 MeV Kr ions indicates that the threshold electronic stopping power for track formation is >15 keV/nm for Xe ions.

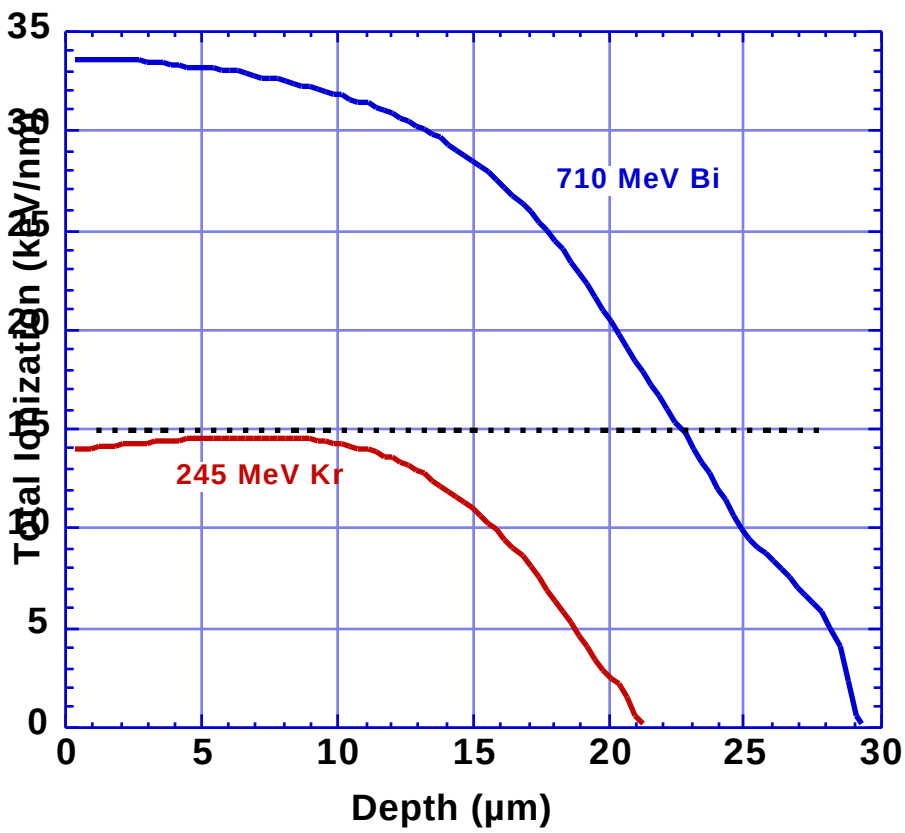

Fig. 4. Comparison of the electronic stopping powers for swift heavy ions in Si_3N_4.

DISCUSSION

In three previous studies of SiC irradiated with swift heavy ions [3-5], there was no evidence for ion track formation. Krstic and coworkers did not observe any swelling in SiC irradiated with 72 MeV I^+ ions (peak electronic stopping power of ~15 keV/nm) up to fluences as high as $1x10^{17}/cm^2$ [4]. Lhermitte-Sebire et al. [3] did not observe evidence for track formation in SiC irradiated with 5.5 GeV Xe ions, where the maximum calculated electronic stopping power was 21.9 keV/nm at a depth of 390 µm. A recent positron annihilation study did not observe evidence for amorphization in SiC irradiated at 300 K with 246 MeV Kr ions (maximum S_e=14.5 keV/nm) up to a fluence of $1x10^{14}$ ions/cm^2 [5]. The present study indicates that track formation does not occur in SiC for electronic stopping powers as high as 34 keV/nm. We are not aware of any previous studies of track formation in AlN or Si_3N_4.

Latent tracks were registered in Si_3N_4, which has the lowest thermal conductivity among the 3 ceramics listed in Table 1. This implies that the observations in this investigation may be interpreted in the framework of the thermal-spike model. The basic assumption of the thermal-spike model connects the latent track formation with quenching of molten matter along the ion path [1,9-11]. Since the experimentally determined value is a track size, R_0, the applicability of approach is usually concluded from the comparison of measured and calculated values of R_0. In the microscopic transient thermodynamic model [9-11] it can be done by solving two coupled equations with one only free parameter – the electron-lattice mean free path $\lambda = (D_e\tau_e)^{1/2}$, where D_e is the thermal electron diffusivity and τ_e the electron-lattice interaction time. This parameter λ is determined by fitting the experimental radii found for a variety of specific inelastic energy loss values S_e,. Since track radii were only observed for one ion beam energy in the present study (710 MeV Bi ions incident on Si_3N_4), further studies using additional ion beams are needed before a quantitative evaluation of the suitability of the thermal spike model can be made.

The alternative phenomenological track formation model proposed by Szenes [12,13] assumes a Gaussian temperature distribution within the ion track. The model predicts that track formation consists of two stages: a low energy deposition regime where the track radius is given by R_0^2~ln S_e, and a higher energy deposition regime where R_0^2~S_e (linear regime). The low-energy regime is associated with the so-called velocity effect: low-velocity ions induce tracks more effectively for a given S_e. The linear regime of track formation has been observed to occur for many insulators over a wide range of electronic stopping powers. Our previously published data on track radii in $MgAl_2O_4$ irradiated with Kr and Xe ions [2] are consistent with the relation summarized above: R=1.0 nm for S_e=16 keV/nm (Kr ions) and R=1.3 nm for S_e=26 keV/nm (Xe ions). In these two cases, the ratio of R_0^2/S_e varies from 15.4 to 16. Further experiments are required in order to check the validity of the linear regime for Si_3N_4.

CONCLUSIONS

Both SiC and AlN have a very high resistance to ion track damage. No evidence for track formation was obtained in these two materials up to electronic stopping powers of 34 keV/nm (710 MeV Bi ions).
Ion tracks are visible in Si_3N_4 irradiated with 710 MeV Bi ions for electronic stopping powers above ~15 keV/nm. Ion tracks were not observed in Si_3N_4 irradiated with 245 MeV Kr ions (maximum electronic stopping power of 14.5 keV/nm). Preliminary analysis of the ion tracks in Si_3N_4 suggests that the track center may be amorphous. Further experimental data obtained with different ion beams are needed to determine whether the thermal spike model or the phenomenological model proposed by Szenes is a more appropriate description of the ion track creation process.

Acknowledgements

This research was sponsored in part by the Office of Fusion Energy Sciences, U.S. Department of Energy under contract DE-AC05-00OR22725 with UT-Battelle, LLC and by the Russian Foundation for Basic Research, grant N 00-02-16559.

REFERENCES

1. M. Toulemonde, S. Bouffard, and F. Studer, Nucl. Instr. Meth. B **91**, 108 (1994).
2. S.J. Zinkle, Hj. Matzke, and V.A. Skuratov, in *Microstructural Processes During Irradiation*, MRS Symposium Proceedings, edited by S.J. Zinkle, G.E. Lucas, R.C. Ewing, and J.S. Williams (Materials Research Society, Warrendale, PA, 1999), Vol. 540, p. 299.
3. I. Lhermitte-Sebire, J. Vicens, J.L. Chermant, M. Levalois, and E. Paumier, Philos. Mag. A **69** (2), 237 (1994).
4. V.D. Krstic, M.D. Vlajic, and R.A. Verrall, Key Engineering Materials **122-124**, 387 (1996).
5. L. Liszkay, K. Havancsák, M.-F. Barthe et al., in *Proc. 12th International Conference on Positron Annihilation,* Munich, Germany, August 6-12, 2000, in press.
6. J.F. Ziegler, J.P. Biersak, and U. Littmark, *The Stopping and Range of Ions in Solids* (Pergamon Press, New York, 1985).
7. T. Yano and T. Iseki, J. Nucl. Mater. **203**, 249 (1993).
8. C-M Wang, X. Pan, M. Rühle, F.L. Riley, and M. Mitomo, J. Mater. Sci. **31**, 5281 (1996).
9. M. Toulemonde, J.M. Costantini, Ch. Dufour et al., Nucl. Instr. Meth. B **116**, 37 (1996).
10. A. Meftah, M. Djebara, N. Khalfaoui et al., Mater. Sci. Forum **248-249**, 53 (1997).
11. M. Toulemonde, Ch. Dufour, A. Meftah, and E. Paumier, Nucl. Instr. Meth. B **166-167**, 903 (2000).
12. G. Szenes, Phys. Rev. B **51** (13), 8026 (1995).
13. G. Szenes, Nucl. Instr. Meth. B **116**, 141 (1996).